Gasoline flame behavior at elevated temperature and pressure

Golnoush Ghiasi, Irufan Ahmed[1], Nedunchezhian Swaminathan*

Cambridge University Engineering Department, Trumpington Street, Cambridge, UK, CB2 1PZ

(Submitted to Fuel, Nov. 23, 2017, revised Oct. 16, 2018, Accepted October 23, 2018)

Abstract

Freely propagating laminar premixed flames of stoichiometric mixtures of gasoline surrogate and iso-octane with air are computed using three chemical kinetics mechanisms of varied complexity and detail. A good agreement of the computed burning velocities with past experimental data is observed. The burning velocities of these mixtures at temperature of $850 \leq T \leq 950$ decrease with pressure up to about 3 MPa and starts to increase beyond this pressure. This contrasting behavior is related to the role of pressure dependent reaction involving OH and the influence of this radical on the fuel consumption rate. The results suggest that the overall order of the combustion reaction is larger than two at pressures higher than 3 MPa. Hence, one must be cautious in extending the commonly used laminar flame speed correlation with pressure to thermo-chemical conditions of interest for future engines.

Keywords: Gasoline surrogate, Iso-octane, Laminar burning velocity,

*Corresponding author

Email address: ns341@cam.ac.uk (Nedunchezhian Swaminathan)

[1]Currently in Ricardo plc., Shoreham-by-Sea, UK

1. Introduction

The emission legislation for automobile engines are becoming increasingly stringent to curtail environmental impact of fossil fuel combustion in these engines. This drives a search for finding new combustion technologies that would offer cleaner and efficient combustion with high thermal efficiency and very low emissions of NO_x, soot and other pollutants. Homogeneous Charge Compression Ignition (HCCI) and Premixed Charge Compression Ignition (PCCI) technology with low NO_x emission and about 10 to 15% improvement in fuel efficiency are promising alternatives to current IC engine combustion technologies [1]. However, maintaining this performance over a broad range of operating conditions (or loads) can be challenging. This is because the expected pressure and temperature conditions required for these combustion concepts can be larger than those in the conventional engines. For example, the in-cylinder pressure peak can reach up to 11.5 MPa with engine boost system [1] for the above alternative combustion concepts. The SKYACTIV-G engines from Mazda operates with high compression ratio and spark controlled compression ignition (SCCI) using gasoline fuels. The next generation, SKYACTIV-X, is projected to perform at 50% efficiency and a reduction in fuel consumption by about 20% [2]. Although the autoignition is accepted to be the mechanism for PCCI/HCCI engines, the use of spark is required to control engine performance over the wide range of load conditions as demonstrated by the Mazda engine. Thus, the flame propagation mechanism and its behaviour under conditions of interest for these engines need

to be explored and understood. Despite the practice demonstrated through SKYACTIVE-G engines, the combustion characteristics and its interaction with turbulence at such high pressure condition can be quite different from those in conventional conditions and are yet to be investigated in detail.

The recent advances in computational hardware, methodologies, and mathematical modelling techniques for turbulent combustion are lending computational fluid dynamics (CFD) as an important tool for developing modern engines. Thus, the CFD simulations and analysis of turbulent reacting flows are embraced by OEMs as an integral part of their engine degin processes. The state-of-the-art of turbulent combustion modellings for multi-dimensional in-cylinder flow analysis were reviewed in earlier studies remarking that the mathematical models will have adequate fidelity if their parameters were closely tied to the physics of the problem [3, 4]. Such models are needed to investigate new combustion concepts involving fuel-lean homogeneous and stratified charge mixtures. This is because the in-cylinder combustion of these mixtures can include strong spatio-temporal variations of turbulence-chemistry interaction and competing effects of flow and thermo-chemistry. Hence, the models should be able to adopt to these changes inherently. This is possible only if the model parameters are related closely to the background physics.

It is well accepted that the laminar burning velocity, S_L, is an essential parameter to determine the fuel burn rate [5] and consequently the power output and efficiency. Also, it is involved in almost all of the sophisticated turbulent combustion models for premixed and partially premixed charges [6]. This fundamental quantity varies with pressure, p, temperature, T, and equiva-

lence ratio of the fuel-air mixture. The pressure and temperature dependence of S_L is typically represented using a power law expression:

$$\frac{S_L}{S_{L,0}} = \left(\frac{T}{T_0}\right)^{\alpha} \left(\frac{p}{p_0}\right)^{\beta}, \tag{1}$$

where $S_{L,0}$ is the laminar burning velocity at p_0 and T_0 for a given equivalence ratio, ϕ. The exponents α and β can vary with ϕ [7, 5] and are obtained using extensive measurements. The laminar burning velocity at $p_0 = 1$ bar and $T_0 = 298$ K is well investigated for simple hydrocarbons and hydrogen fuels [8]. The variation of laminar burning velocities for fuel-air mixtures of iso-octane, n-heptane, primary reference fuels (PRF) and gasoline with equivalence ratio at elevated mixture temperature and pressure was also investigated in the past [9, 10, 11]. The maximum pressure and temperature of the fuel-air mixture were limited to (1 MPa, 473 K) in [10], (2.5, 373) in [9] and (0.6, 358) in [11]. All of these studies showed that β in Eq. (1) takes a negative value implying that S_L decreases with increase in p for a given mixture temperature and equivalence ratio.

The classical theory of premixed flames suggests that the mass burning rate per unit area $\dot{M} = \rho_u S_L$, where ρ_u is the reactant density, varies as the square root of fuel consumption rate [12], which was originally identified by Zeldovich and Frank-Kamenetskii [13]. This theory suggests that $\beta = (n-2)/2$, where n is the overall order for the global combustion reaction. For most hydrocarbon stoichiometric and fuel-lean combustion in air n is typically smaller than 1.2 [14] and thus β is smaller than -0.4, while the experimental measurements suggest that $\beta \sim -0.5$ [15]. For the PRFs-air mixtures, this exponent was shown to be about -0.3 over the pressure varying from 1 to 10 bar with mixture temperature ranging between 358

to 450 K [16, 9, 17]. The pressure dependence of S_L arise because of the fundamental importance of the pressure-sensitive chain reactions involved in the combustion chemistry - the relative importance between the chain branching and termination reactions changes with pressure [14]. These kind of analyses are typically done using lower hydrocarbon such as methane for example and thus, one can ask if these findings would hold or not for higher hydrocarbons specifically for iso-octane or gasoline combustion.

The iso-octane is one of the PRFs and thus it is important to know the pressure dependence of its laminar burning velocity at thermo-chemical conditions expected in future engines. The reactant mixture temperature ranging from 850 to 950 K at pressure ranging from 3 to 4 MPa are of interest here because the low-temperature and high-temperature oxidations of fuel were observed to occur at these conditions in a dual-fuel stratified PCCI engines [1]. Thus, the laminar flame behaviours for stoichiometric mixtures of gasoline surrogate and iso-octane with air at the above conditions are of interest here. Specifically, the objective is to find an answer to the question: is there a monotonic decrease of S_L with p as noted above or something else for these mixtures at thermo-chemical conditions of interest here? As discussed earlier S_L is a central quantity for many combustion models and thus it is important to understand its behaviour at conditions relevant for next generation of internal combustion engines.

This objective is addressed by performing laminar flame computations using the state-of-the art comprehensive chemical mechanisms, validated well in previous studies, for the reactant mixtures of interest here. The detail on the laminar flame calculations and the chemical kinetics mechanisms used

are discussed in the next section. Results are presented in section 3 and conclusions are summarised in the final section.

2. Computational Detail

The conservation equations for mass, momentum, energy and various chemical species mass fractions involved in the combustion chemistry are solved for a freely propagating one-dimensional laminar premixed flame. The specific forms of these equations and the associated boundary conditions are well known and they can be found, for example in [18]. The laminar mass burning flux, $\dot{M}$ and hence S_L, appears as the eigenvalue of the system of above equations and thus the laminar burning velocity is computed as a part of the solution. The coupled algebraic equations resulting from the discretisation of these conservation equations are solved using an adaptive gridding technique in PREMIX code of the CHEMKIN-Pro software and the accuracy of the solution is controlled by limiting the parameters for gradient and curvature of the spatial variations of temperature and various species mass fractions to be lower than set limits. These parameters were specified to be about 0.01 for both (gradient and curvature) parameters. The molecular transport is modelled using mixture-averaged formulation available in the software to save computational efforts since the difference in the results with this and multi-component diffusion velocity formulations were observed to be very small for the conditions investigated in this study. As noted in the previous section, behaviours of laminar premixed flames at relatively high temperature and pressure are of interest and thus the reactant temperatures range from 850 to 950 K for pressures varying from 30 to 40 bar. These condi-

tions are chosen based on the expected in-cylinder pressure and temperature of mixture for the next generation of internal combustion engines [19, 20]. The combustion chemistry is modelled using three different mechanisms of varied complexity described next.

2.1. Chemical mechanisms

One of the earlier detailed iso-octane mechanisms was developed by Warnatz [21], which was upgraded subsequently by Westbrook et al. [22] to investigate engine knock. This mechanism contained 765 reversible reactions involving 212 species. Curran et al. [23] developed a comprehensive mechanism involving about 860 species and 3600 reactions for combustion of iso-octane-air mixtures for reactant temperature up to 1700 K and pressure ranging from 0.1 to 4.5 MPa. Other mechanisms developed in the past to study laminar flame speeds of iso-octane and other hydrocarbons were reviewed by Ranzi et al. [17].

Mehl et al. [24] developed a comprehensive mechanism involving 6000 reactions and 1550 species for combustion of gasoline surrogate mixtures by merging n-heptane, iso-octane and toluene mechanisms. This comprehensive mechanism was validated for reactant temperature as high as 1200 K and pressure of 5 MPa and thus it is useful to investigate combustion phenomena at engine relevant conditions. This mechanism can also be used to investigate combustion of pure iso-octane (without species like n-heptane or toluene and other trace species) systematically at conditions of interest for this study - reactant temperature varying between 850 to 950 K and pressure up to 4 MPa. The mechanism of Curran et al. [23] is a sub-mechanism of the comprehensive set of Mehl et al. [24]. For comparison purposes, two skeletal

mechanisms for combustion of iso-octane in air are used. A skeletal mechanism that involves 49 reactions and 29 species was proposed by Hasse et al. [25] and is referred as Mech-1 in the discussion below. The second skeletal mechanism by Pepiot-Desjardins and Pitsch [26], referred to as Mech-2 below, is considerably larger as it has 109 species and 393 reactions. The comprehensive mechanism of Mehl et al. [24] is referred as Mech-3 in the discussion below. Details of these mechanisms, such as rate parameters, third body collision efficiency factors, etc., are available in the respective studies cited above. These three mechanisms are used to investigate the behaviour of S_L at thermo-chemical conditions of interest here.

Stanglmaier et al. [27] reported that the laminar burning velocity of gasoline was considerably different from that of iso-octane at higher pressure and temperature based on their experiments. Thus, gasoline surrogate, in addition to iso-octane, mixture is also considered for this study. The gasoline surrogate used here has a RON (Research Octane number) of about 91 and is a mixture of iso-octane (57% by volume), n-heptane (16%), toluene (23%) and 1-pentene (4%), which is taken from the study of Kukkadapu et al. [28]. Note that this RON value is higher than the optimum RON value (about 70) typically considered for PCCI or HCCI applications [29]. Also, fuels with RON value as high as 90 can also be employed but with a high EGR (exhaust gas recirculation) to limit high temperature in order to avoid knocking, which is projected to be used in SKYACTIV-X engines from Mazda [2].

3. Results and discussion

3.1. Validation cases

Experimental data for S_L of stoichiometric iso-octane-air mixture at high temperature and pressure (about 900 K and 3 to 4 MPa) are not available in the literature and thus a direct comparison of the values computed in this study cannot be made. The available flame speed measurements are carefully selected to validate the chemical mechanisms and the approach used for this study. Since the interest is on S_L at elevated temperature and pressure, the experimental data are chosen systematically for validation and the results are shown in Fig. 1. The measurements were taken by Bradley et al. [16], Lawes et al. [30], Mandilas et al. [31], Jerzembeck et al. [9], Kelley et al. [32], and Galmiche et al. [10]. The maximum pressure and temperature explored in these studies are 2.5 MPa and 473 K respectively. These values are nearly 50% of the maximum values of interest for this study.

Galmiche et al. [10] showed that there are significant discrepancies between the measured and computed laminar burning velocity of iso-octane-air mixtures. They used the, Mech-1, mechanism of Hasse et al. [25] and another mechanism from Jerzembeck et al. [9]. This second mechanism is similar to the Mech-2 mechanism used here. It is also important to note that there are significant discrepancies in the experimental data shown in Fig. 1. For example at $T_u = 373$ K and 10 bar there is a difference of about 15% between the results of Galmiche et al. [10] and Jerzembeck et al. [9]. There is even some difference in S_L values measured by a the same research group for atmospheric pressure at $T_u = 450$ K and for 5 bar at $T_u = 400$ K. These differences are due to the uncertainties associated with the difference in the

experimental setup and methodologies employed [10, 33]. The results shown in Fig. 1 are in agreement with measurements reported in past studies and also this comparison improves for the comprehensive mechanism of Mehl et al. [24], Mech-3, in general. This echoes the conclusion of Galmiche et al. [10] that elaborate mechanisms are required for iso-octane combustion. It is quite likely that this observation also applies to gasoline surrogate and PRF mixtures and the published S_L measurements for these mixtures are typically available for temperatures ranging from 298 to 400 K at atmospheric pressure [34]. Thus, further measurements at elevated pressures of interest for future engines are required.

Two commonly used flame speed correlations are also shown in Fig. 1 for comparison purpose. The flame speeds at atmospheric pressure are predicted quite well by these correlations. Also, they capture the flame speed variations with p for various T_u up to 10 bar and they severely overestimate S_L for higher pressures. The correlation CoR1 from [35] underestimates S_L for $T_u \geq 400$ K and it over estimates for $T_u = 353, 360$ and 373 K as shown in Fig. 1. The predictions by correlation CoR2 proposed by Metghalchi and Keck [7] given in Eq. (1) are similar to CoR1. The flame speed values computed using Mech-2 are close to those obtained for Mech-3 up to a pressure of 10 bar for all T_u shown in Fig. 1. However, S_L values from the Mech-2 become gradually smaller than those from the Mech-3 as p increases beyond 10 bar. More experimental measurements of the laminar flame speeds for higher pressures are required for full assessment of these mechanisms. However, one must note that the pressure dependent elementary reactions can become important at elevated pressures and these reactions are present only in comprehensive

mechanisms. Their influences on autoignition delay times were noted in previous studies [28] and we shall explore their role on flame propagation at the conditions considered for this study.

3.2. Flame speed and structure at elevated T and p

If the autoignition is likely to occur for a given T_u and p then a flame solution ceases to exists leading to numerical divergence while solving the required conservation equations with convection, diffusion and reaction balance for flame propagation. This is because the ignition delay time is of the same order as the characteristic flame time when the autoignition is likely to occur [36]. The conditions, T_u and p, at which the numerical divergence occurs are plotted in Fig. 2 for the two mechanisms, Mech-2 and Mech-3. The region below each curve allows a flame solution and the region above is for autoignition (marked as "No Flame" in the figure). The results are shown for stoichiometric iso-octane and air mixture using both the Mech-2 and Mech-3 mechanisms. The gasoline surrogate mixture requires a comprehensive mechanism and thus the results obtained using the Mech-3 are shown for this mixture. The adiabatic compression curve is also shown for reference and this curve is obtained using $\gamma = 1.3$ which is an average value of γ over the temperature range of $298 \leq T \leq 1500$ K [37]. The onset of the autoignition is sensitive to the detail in the chemical kinetics mechanism used. The skeletal mechanism, Mech-2, suggests autoignition to occur above 45 bar for $T \geq 800$ K whereas the comprehensive mechanism, Mech-3, allows flame solution as seen in Fig. 2. Some of these conditions are suggested to be autoignition by the skeletal mechanism but the comprehensive mechanism suggests flame propagation. The chemical kinetic description of iso-octane

combustion requires an elaborate mechanism as concluded by Galmiche et al. [10] and thus further results discussed below are for the Mech-3, the comprehensive mechanism of Mehl et al. [24].

Figure 3 shows the spatial variations of temperature and few major and minor species across the computed flames for 40 bar pressure and two reactant temperaures, 900 and 950 K. The distance through the flame is normalised using the respective thermal thickness, δ_{th}, as $x = (\widehat{x} - \widehat{x}_0)/\delta_{th}$, where $\widehat{x}$ is the dimensional distance through the flame and $\widehat{x}_0$ corresponds to the location for $c = (T - T_u)/(T_b - T_u) = 0.5$. The thermal thickness is defined as $\delta_{th} = (T_b - T_u)/|dT/d\widehat{x}|_{\max}$ and the product temperature is denoted using T_b. Only a small part of the domain is shown in this figure to emphasis the variations around the flame. There is a very sharp rise in T and its spatial variation typical of a laminar premixed flame. The mole fraction of C_8H_{18} starts from about 9.2×10^{-3} and drops to zero at $x = 0$ for $T_u = 900$ K as shown in the figure. The variations of other species shown in this figure are typical for laminar premixed flames. When the reactant temperature is increased to $T_u = 950$ K there is a substantial change in the variation of iso-octane mole fraction. Its value drops by about 18.5% at $x \simeq -25$ compared to the case with $T_u = 900$ K although the equivalence ratio is the same for these two cases. Also, there is a quick drop in the iso-octane mole fraction value as seen in figure 3. Furthermore, there is an increase in H2O mole fraction for $x \leq 0$ when the reactant temperature is 950 K. The atomic hydrogen mole fraction is substantially larger but the CH2O variation has not changed. The strong variation seen for the iso-octane and atomic hydrogen mole fractions suggests that the low-T chemistry becomes important when

$T_u = 950$ K. Nevertheless, the variations of temperature and various species mole fractions shown in Fig. 3 demonstrate that there is a high T flame structure with its peak heat release occurring at about $x = 0$.

The burning rate mass flux $\dot{M} = \rho_u S_L$ is directly related to the fuel consumption rate per unit volume, $\dot{\omega}_f$, integrated across the flame, ie., $\dot{M} = \int \dot{\omega}_f \quad dx/Y_{f,u}$. It is quite easy to verify this by integrating the fuel mass fraction transport equation across the steady laminar flame and applying the boundary conditions. The variation of $\dot{M}$ normalised by its value at $p_0 = 1$ bar is plotted against (p/p_0) in Fig. 4. Logarithmic scales are used to emphasis a power-law behaviour, ie., $\dot{M} \sim p^m$, which implies that $\beta = (m - 1)$ (see Eq. 1). This gives $m = n/2$, where n is the overall order of the global combustion reaction. The generally accepted value of $\beta \simeq -0.5$ for most of the hydrocarbons suggests that $m = 0.5$, which is different from $m \simeq 0.75$ deduced from the results in Fig. 4 for $p \leq 10$ bar. However, this computationally deduced value of 0.75 is close to the experimental value of $m \simeq 0.78$ reported in [35] for iso-octane combustion with air. A close scrutiny of the results in the figure suggests that the value of m is smaller for p larger than 10 bar but it starts to increase beyond about 33 bar. This increase is observed to be negligible for 850 and 900 K iso-octane mixture but it is appreciable for iso-octane at 950 K and also for the gasoline surrogate mixtures shown in the figure. This behaviour clearly suggests that m, thus the overall order of the combustion reaction, varies with pressure. It is also worth to note that these changes are observed for pressures well within the range of validity (up to 50 bar) for the chemical mechanism, Mech-3.

One can deduce the flame speed, S_L, variations with p using the mass

burning rate results discussed above. If one needs to have a negative pressure dependence (ie., $\beta < 0$ for Eq. 1) then m must be less than 1 (see above) but the sharp increase in the slope of the curves shown in Fig. 4 suggests that $\beta > 0$. Indeed, this is observed in Fig. 5 showing the normalised flame speed variation with normalised pressure for both iso-octane and gasoline mixtures. The upward turn around 36 bar for the iso-octane mixture at 950 K shows that $\beta > 0$. Such a behaviour is seen for the gasoline surrogate mixtures also. The insets in Fig. 5 depicts the variation of β with $\ln(p/p_0)$ showing that the laminar flame speed increases with pressure beyond about 33 bar for the conditions considered in this study, which are of interest for alternative engine combustion technologies. This behaviour of S_L increasing with p is in contrast to the behaviour at relatively lower pressures and this is because of the change in the behaviour of pressure dependent reaction producing OH as discussed in the next section. The increase in S_L with p was also reported in the past for stoichiometric methane-air mixture at $T_u = 1450$ K and this behaviour was suggested to come from autoignition events [38], for which S_L definition is quite ambiguous. The current observation is for premixed flames and is because of the change in the role of pressure dependent reaction involving OH.

4. Discussion

The fuel, for example iso-octane, is consumed by a number of elementary reactions involving radicals and intermediate species and fuel pyrolysis. Thus, the fuel consumption rate is the sum of net rates of these elementary reactions, ie., $\dot{\omega}_f = W_f \sum \dot{\omega}_i$, where W_f is the molecular mass of the fuel

Table 1: First 15 most important reactions involving iC_8H_{18}

Number	Reaction
3214	$iC_8H_{18} = YC_7H_{15} + CH_3$
3215	$iC_8H_{18} = PC_7H_{15} + CH_3$
3216	$iC_8H_{18} = TC_4H_9 + IC_4H_9$
3217	$iC_8H_{18} = NEOC_5H_{11} + IC_3H_7$
3218	$iC_8H_{18} + H = AC_8H_{17} + H_2$
3219	$iC_8H_{18} + H = BC_8H_{17} + H_2$
3220	$iC_8H_{18} + H = CC_8H_{17} + H_2$
3221	$iC_8H_{18} + H = DC_8H_{17} + H_2$
3222	$iC_8H_{18} + O = AC_8H_{17} + OH$
3224	$iC_8H_{18} + O = CC_8H_{17} + OH$
3226	$iC_8H_{18} + OH = AC_8H_{17} + H_2O$
3227	$iC_8H_{18} + OH = BC_8H_{17} + H_2O$
3228	$iC_8H_{18} + OH = CC_8H_{17} + H_2O$
3229	$iC_8H_{18} + OH = DC_8H_{17} + H_2O$
3230	$iC_8H_{18} + CH_3 = AC_8H_{17} + CH_4$

species. Analysing these reactions by rank ordering them according to their contribution to the total fuel consumption rate allows us to identify the first 15 most important reactions involving iC_8H_{18} and these reactions are listed in Table 1. The reaction numbers listed in the table are those in the chemical mechanism [24]. The first 4 are fuel pyrolysis and the other reactions represent the fuel-attack by radicals and an intermediate, CH_3. The net rates of these reactions integrated across the flame are shown in Fig. 6 for both

iC_8H_{18} and gasoline surrogate mixtures at four different pressures, 35, 40, 45 and 50 bar, and two reactant temperatures, 850 and 900 K. It is apparent that the relative contributions of these reactions to the fuel consumption rate remain almost the same for both iso-octane and gasoline mixtures for both temperatures. Generally, the rates of these reactions increase with reactant temperature as one would expect. The rates of reactions 3214 to 3224 and 3230 either decrease or remain more or less constant with pressure and thus they are not responsible for the increase in S_L (or fuel consumption rate) with p.

The rates of reactions involving OH, numbered 3226 to 3229 in Table 1, standout for all the cases shown in Fig. 6 and also their relative contributions increase with p, implying that these reactions are responsible for the sharp increase in S_L and $\dot{M}$ with p. All of these elementary reactions listed in Table 1 are bimolecular and so their rates do not depend on pressure. Hence the increase in their net rates with p should come through the relative role of pressure dependent reactions involving OH. Typically, pressure dependent reactions are chain terminating reaction, ie., they consume radicals like OH. A careful scrutiny of the chemical mechanism identifies a pressure dependent OH-producing reaction, $H_2O_2(+M) \longleftrightarrow OH + OH(+M)$, which is numbered as 16 in the mechanism [24].

Figure 7 shows the variations of net rates with p for reactions 3226 to 3229 and 16. A positive value implies that net reaction is in the forward direction and a negative value implies the backward direction. These reaction rates are integrated across the flame and they are shown for the gasoline mixture at 900 K. These results are consistent with the results in the Figure 6.

The sum of these net rates for reactions 3226 to 3329 is also shown in the Figure 7, marked as "Total". It is quite clear that the consumption of iC_8H_{18} increases with p and this increase is because of the change in the role of reaction 16, which gradually shifts to the right as the pressure increases implying that this reaction changes from OH-consuming to OH-producing reaction, the net rate of this reaction changing from negative to positive values as in Figure 7. A similar behaviour is seen for other temperatures in the range, 850 to 950 K, considered for this study. Thus, the increase in S_L with p is because of the change in the role of reaction 16. Since this reaction is pressure dependent and the collision partner M includes all the species except H_2O_2 in the mixture, the overall order of the combustion reaction is also changing with p.

5. Summary and Conclusion

Freely propagating laminar premixed flames of stoichiometric mixtures of gasoline surrogate and iso-octane with air are computed in the view to understand their structures and burning velocities at conditions which are of interest for future IC engine combustion technologies such as PCCI and HCCI. The reactant temperature and pressure of interest for this study are $850 \leq T_u \leq 950$ K and 3 to 4 MPa. These flames are computed using CHEMKIN-PRO software and the combustion kinetics are modelled using three different mechanism of varied level of detail and complexity. These mechanisms are validated using carefully selected experimental data of burning velocity for iso-octane from several past studies. It is observed that elaborate mechanisms are required to capture iso-octane combustion and to

predict its laminar burning velocity as noted by Galmiche et al. [10]. This observation also applies for gasoline surrogate mixtures.

The computations using a comprehensive mechanism [24], denoted here as Mech-3, suggest that propagating flames exists for the temperature (850 to 950 K) and pressure up to 80 bar whereas a skeletal mechanism [26], denoted as Mech-2, yield no flame for $T = 900$ K and $p > 45$ bar as shown in Fig. 2 suggesting possible autoignition. The results obtained using the comprehensive mechanism, which is valid up to 50 bar, are analysed in detail. The burning velocity of both stoichiometric iso-octane and gasoline surrogate mixtures decreased with pressure for the temperature range of interest ($850 \leq T \leq 950$ K) and these results, both flame structure and burning velocity, are consistent with the classical theory of premixed flames. The pressure exponent, $m \simeq 0.75$, for the mass burning rate flux calculated using the laminar flame results of iso-octane flames up to 30 bar is close to the experimental value of 0.78 [35]. However, this mass flux start to increase quite significantly beyond this pressure for the temperature range investigated and thus the laminar burning velocity increases with pressure. This behaviour is in contrast to that suggested by a commonly used correlation given in Eq. (1) and it ensues for the following reasons. The net rate of pressure dependent reaction $H_2O_2(+M) \longleftrightarrow OH + OH(+M)$ changes progressively from negative towards positive value as the pressure increases suggesting that this reaction changes from OH-consuming to OH-producing reaction. Thus, the rate of iso-octane consumption through reactions 3226 to 3229 in Table 1 involving OH increases with p leading to the observed behaviour (increase) of S_L with p. It is worth noting that this behaviour is for pressures well

within the range of validity for the comprehensive chemical mechanism used in this study. It is imperative that chemical mechanisms validated carefully for pressures up to 100 bar and beyond are of interest in the view of future combustion technologies which may be friendlier to the environment.

It is also important to note that higher hydrocarbons such as iso-octane and gasoline can pyrolyse into smaller hydrocarbons at elevated temperature and also the low-T chemistry can play a role. Thus, the fuel-air mixture approaching the high-T flame may have a number of hydrocarbons of varied reactivity, which are different from the original fuel-air mixture. Hence, carefully conducted experimental investigations are required to shed further lights on the contrasting behaviour of the laminar flame speed with pressure observed in this study.

Acknowledgement

The support from KACST is acknowledged. One of the anonymous reviewer is acknowledged for raising interesting and very useful queries.

References

[1] Inagaki, K., Fuyuto, T., Nishikawa, K., Nakakita, K., Sakata, I. Combustion system with premixture-controlled compression ignition. R& D Review of Toyota CRDL 2006;4(3):35–46.

[2] Mazda Inc. SKYACTIV-X next generation gasoline engine. http://www.mazda.com/en/notification/20180330/ Accessed 10/Oct/2018;.

[3] Haworth, D. C. A review of turbulent combustion modeling for multidimensional in-cylinder cfd. SAE Technical Paper 2005-01-0993 2005;:899–927.

[4] Drake, M., Haworth, D. Advanced gasoline engine development using optical diagnostics and numerical modeling. Proc. Combust. Inst. 2007;31:99–124.

[5] Lindström, F., Ångström, H.-E., Kalghatgi, G., Möller, C. A. An empirical si combustion model using laminar burning velocity correlations. SAE Tech. Pap. 2005-01-2106 2005;.

[6] N. Swaminathan and K. N. C. Bray, Turbulent Premixed Flames, Cambridge University Press, Cambridge, UK, 2011.

[7] Metghalchi, M., Keck, J. C. Burning velocities of mixtures of air with methanol, isooctane, and indolene at high pressure and temperature. Combust. Flame 1982;48:191–210.

[8] Law, C. K. A compilation of experimental data on laminar burning velocities. in: Peters, N., Rogg, B. (Eds.), Reduced kinetic mechanisms for applications in combustion systems, Springer-Verlag, Berlin, 1993, pp. 15–26.

[9] Jerzembeck, S., Peters, N., Pepiot-Desjardins, P., Pitsch, H. Laminar burning velocities at high pressure for primary reference fuels and gasoline: experimental and numerical investigation. Combust. Flame 2009;156:292–301.

[10] Galmiche, B., Halter, F., Foucher, F. Effects of high pressure, high temperature and dilution on laminar burning velocities and Markstein lengths of iso-octane/air mixtures. Combust. Flame 2012;159:3286–3299.

[11] Mannaa, O., Mansour, M., Roberts, W. L., Chung, S. Laminar burning velocities at elevated pressures for gasoline and gasoline surrogates associated with RON. Combust. Flame 2015;162:2311–2321.

[12] Zeldovich, Y. B., Barenblatt, G. I., Librovich, V. B., Makhviladze, G. M., The mathematical theory of combustion and explosions, translated from Russian by D. H. McNeil, Consultants Bureau, New York, 1985.

[13] Zeldovich, Y. B., Frank-Kamenetskii, D. A. A theory of thermal propagation of flame. Acta Physicochim, USSR (Russian) 1938;9:341–350.

[14] Law, C. K., Combustion Physics, Cambridge University Press, 2006.

[15] Turns, S. R., An Introduction to Combustion: Concepts and Applications, second ed., McGraw-Hill, Singapore, 2000.

[16] Bradley, D., Hicks, R. A., Lawes, M., Sheppard, C. G. W., Woolley, R. The measurement of laminar burning velocities and markstein numbers for iso-octaneair and iso-octanen-heptaneair mixtures at elevated temperatures and pressures in an explosion bomb. Combust. Flame 1998;115:126–144.

[17] Ranzi, E., Frassoldati, A., Grana, R., Cuoci, A., Faravelli, T., Kelley, A. P., Law, C. K. Hierarchical and comparative kinetic modeling of

laminar flame speeds of hydrocarbon and oxygenated fuels. Prog. Energy Combust. Sci. 2012;38:468–501.

[18] Smooke, M. D., Giovangigli, V. Formulation of the premixed and non-premixed test problems. in: Smooke, M. D. (Ed.), Reduced Kinetic Mechanisms and Asymptotic Approximations for Methane-Air Flames, Springer-Verlag, Berlin, 1991, pp. 1–28.

[19] Laguitton, O., Gold, M., Kennaird, D., Crua, C., Lacoste, J., Heikal, M. Spray development and combustion characteristics for common rail diesel injection systems. in: IMechE Conference Transactions: Fuel injection systems, Professional Engineering Publishing, London, UK, 2003, pp. 55–72.

[20] Hyvonen, J., Harakdsson, G., Johansson, B. Operating range in a multi cylinder hcci engine using variable compression ratio. SAE paper 011829, JSAE 20030178 2003;.

[21] Warnatz, J. Chemistry of high temperature combustion of alkanes up to octane. Symp. Combust. 1985;20:845–856.

[22] Westbrook, C. K., Warnatz, J., Pitz, W. J. A detailed chemical kinetic reaction mechanism for the oxidation of iso-octane and n-heptane over an extended temperature range and its application to analysis of engine knock. Symp. (International) Combust. 1989;22:893–901.

[23] Curran, H. J., Gaffuri, P., Pitz, W. J., Westbrook, C. K. A comprehensive modeling study of iso-octane oxidation. Combust. Flame 2002;129:253–280.

[24] Mehl, M., Pitz, W. J., Westbrook, C. K., Curran, H. J. Kinetic modeling of gasoline surrogate components and mixtures under engine conditions. Proc. Combust. Inst. 2011;33:193–200.

[25] Hasse, C., Bollig, M., Peters, N., Dwyer, H. A. Quenching of laminar iso-octane flames at cold walls. Combust. Flame 2000;122:117–129.

[26] Pepiot-Desjardins, P., Pitsch, H. An efficient error-propagation-based reduction method for large chemical kinetic mechanisms. Combust. Flame 2008;154:67–81.

[27] Stanglmaier, R., Roberts, C., Mehta, D., Chadwell, C., Corwin, S. J., Watkins, M. Measurement of laminar burning velocity of multi-component fuel blends for use in high-performance SI engines. SAE Tech. Paper 2003-01-3185 2003;.

[28] Kukkadapu, G., Kumar, K., Sung, C.-J., Mehl, M., Pitz, W. J. Autoignition of gasoline and its surrogates in a rapid compression machine. Proc. Combust. Inst. 2013;34:345–352.

[29] Manente, V., Johansson, B., Cannella, W. Gasoline partially premixed combustion, the future of internal combustion engines? Int. J. Engine Res. 2011;12:194–208.

[30] Lawes, M., Ormsby, M. P., Sheppard, C. G. W., Woolley, R. Variation of turbulent burning rate of methane, methanol, and iso-octane air mixtures with equivalence ratio at elevated pressure. Combust. Sci. Technol. 2005;177:1273–1289.

[31] Mandilas, C., Ormsby, M. P., Sheppard, C. G. W., Woolley, R. Effects of hydrogen addition on laminar and turbulent premixed methane and iso-octaneair flames. Proc. Combust. Inst. 2007;31:1443–1450.

[32] Kelley, A. P., Liu, W., Xin, Y. X., Smallbone, A. J., Law, C. K. Laminar flame speeds, non-premixed stagnation ignition, and reduced mechanisms in the oxidation of iso-octane. Proc. Combust. Inst. 2011;33:501–508.

[33] Sileghem, L., Alekseev, V. A., Vancoillie, J., Geem, K. M. V., Nilsson, E. J. K., Verhelst, S., Konnov, A. A. Laminar burning velocity of gasoline and the gasoline surrogate components iso-octane, n-heptane and toluene. Fuel 2013;112:355–365.

[34] Liao, Y.-H., Roberts, W. L. Laminar flame speeds of gasoline surrogates measured with the flat flame method. Energy & Fuels 2016;30:1317–1324.

[35] Gülder, O. L. Correlations of laminar combustion data for alternative S. I. engine fuels. SAE Technical Paper Series, 1984-841000 1984;.

[36] Martz, J. B., Middleton, R. J., Lavoie, G. A., Babajimopoulos, A., Assanis, D. N. A computational study and correlation of premixed isooctane-air laminar reaction front properties under spark ignited and spark assisted compression ignition engine conditions. Combust. Flame 2011;158:1089–1096.

[37] Ceviz, M. A., Kaymaz, I. Temperature and airfuel ratio dependent spe-

cific heat ratio functions for lean burned and unburned mixture. Energy Conv. Management 2005;46:2387–2404.

[38] Habisreuther, P., Galeazzo, F. C. C., Prathap, C., Zarzalis, N. Structure of laminar premixed flames of methane near the auto-ignition limit. Combust. Flame 2013;160:2770–2782.

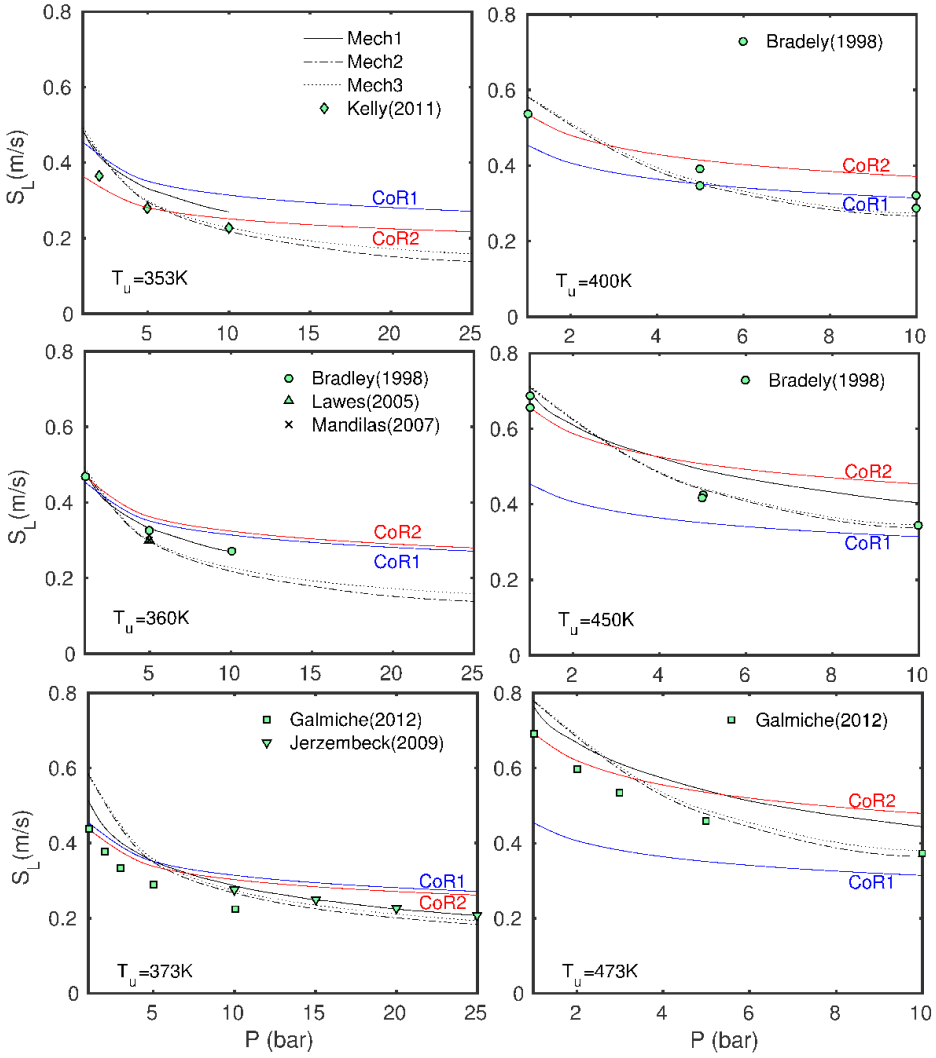

Figure 1: Comparison of measured and computed S_L for stoichiometric iso-octane-air mixtures at various reactant temperature, T_u and pressure. Results are shown for three mechanisms along with commonly used flame speed correlations: Cor1 is from [35], Cor2 is from [7].

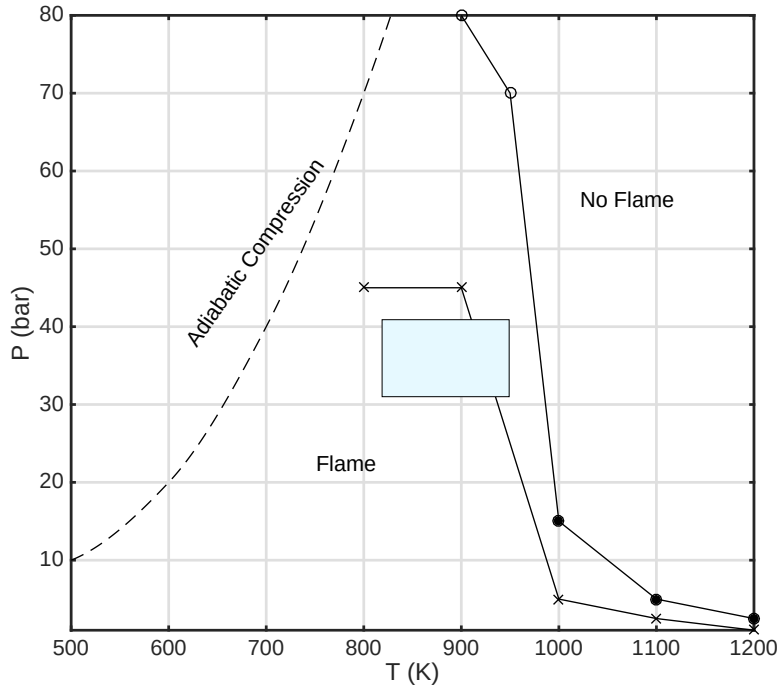

Figure 2: Flame and autoignition regions in T-P space predicted using Mech-2 ($\times$) and Mech-3 (circles) mechanisms for stoichiometric iso-octane and air mixture. The results are also shown for the gasoline surrogate mixture (open circles). The rectangular region marked shows the mixture conditions explored to investigate the flame structure and speed at elevated temperature and pressure.

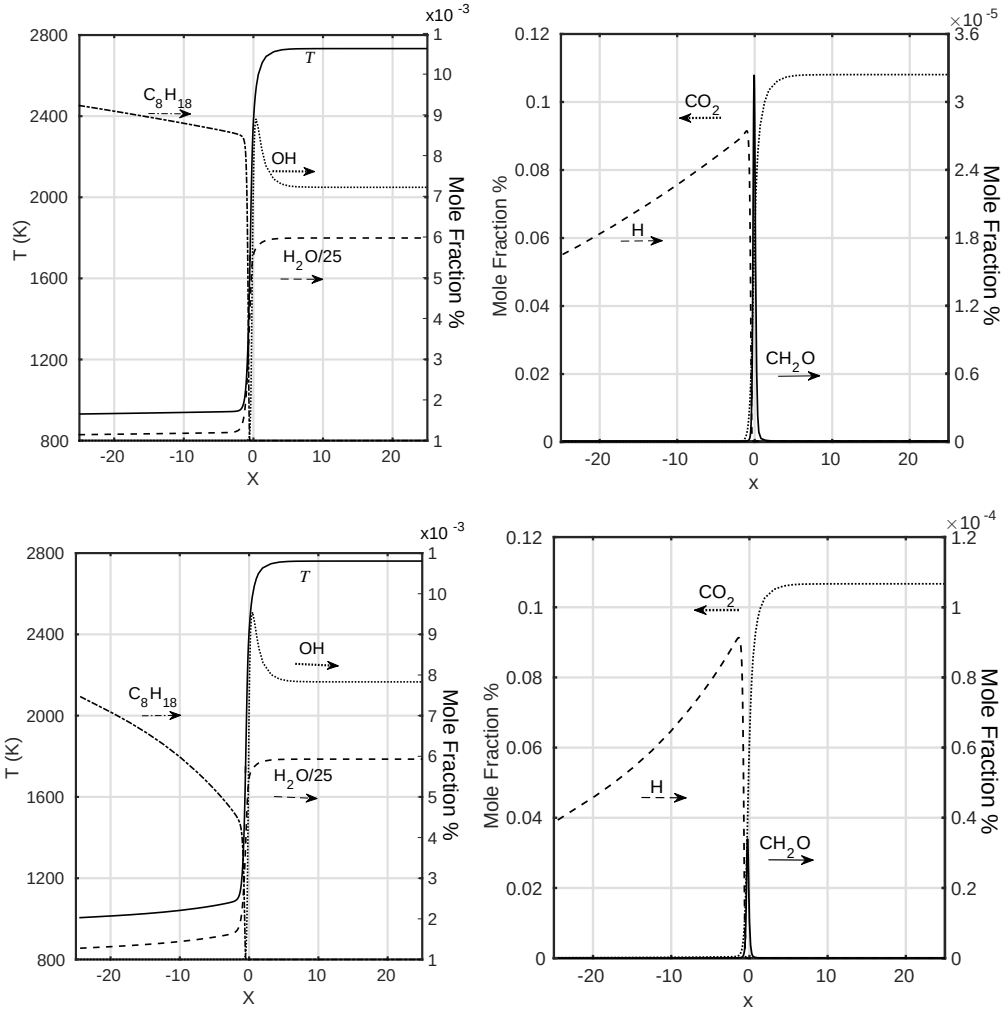

Figure 3: Spatial variation of T and few selected species mole fractions across the flame for $T_u = 900$ K (top row) and 950 K (bottom) at 40 bar.

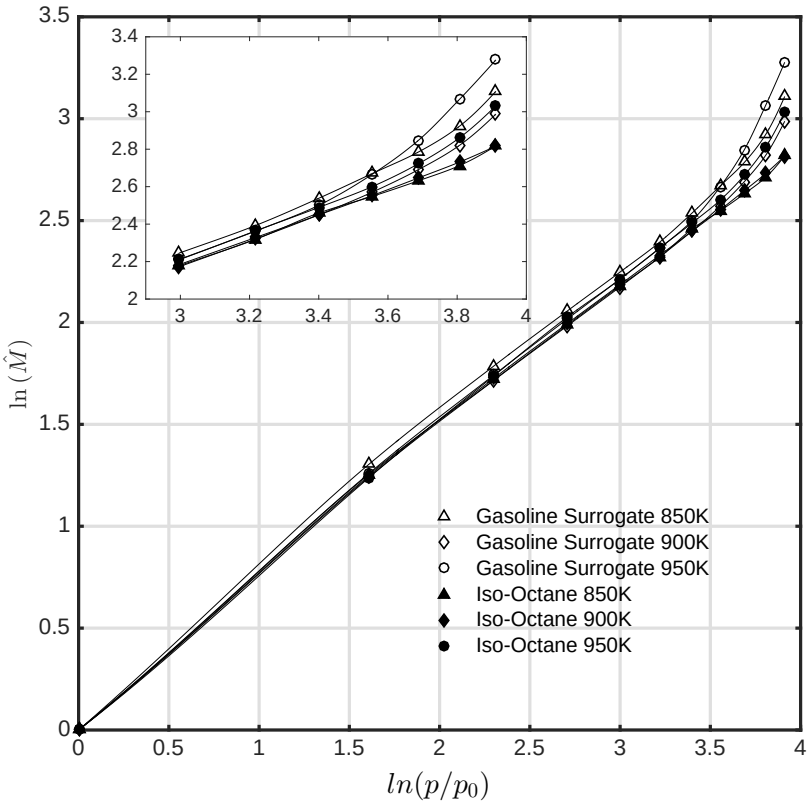

Figure 4: Variation of normalised burning rate mass flux with pressure for iso-octane and gasoline surrogate mixtures at three different temperatures.

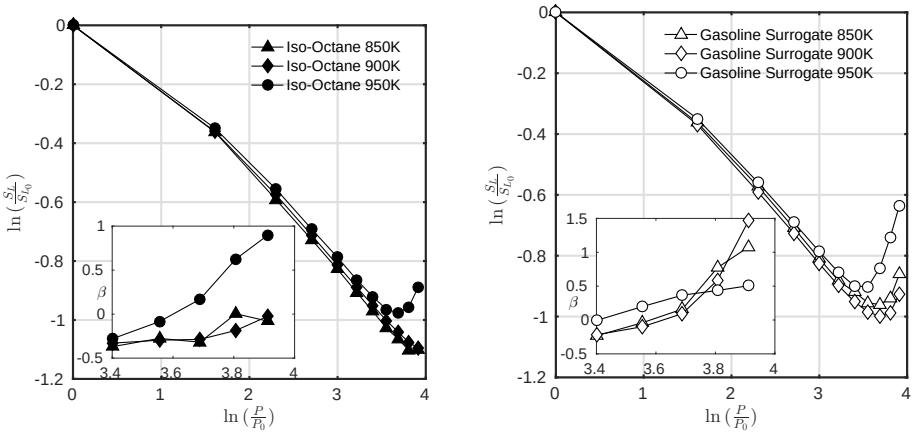

Figure 5: Variation of normalised flame speed with pressure for stoichiometric iso-octane (left) and gasoline surrogate mixtures at three different temperatures. The inset shows the variation of β with $\ln(p/p_0)$.

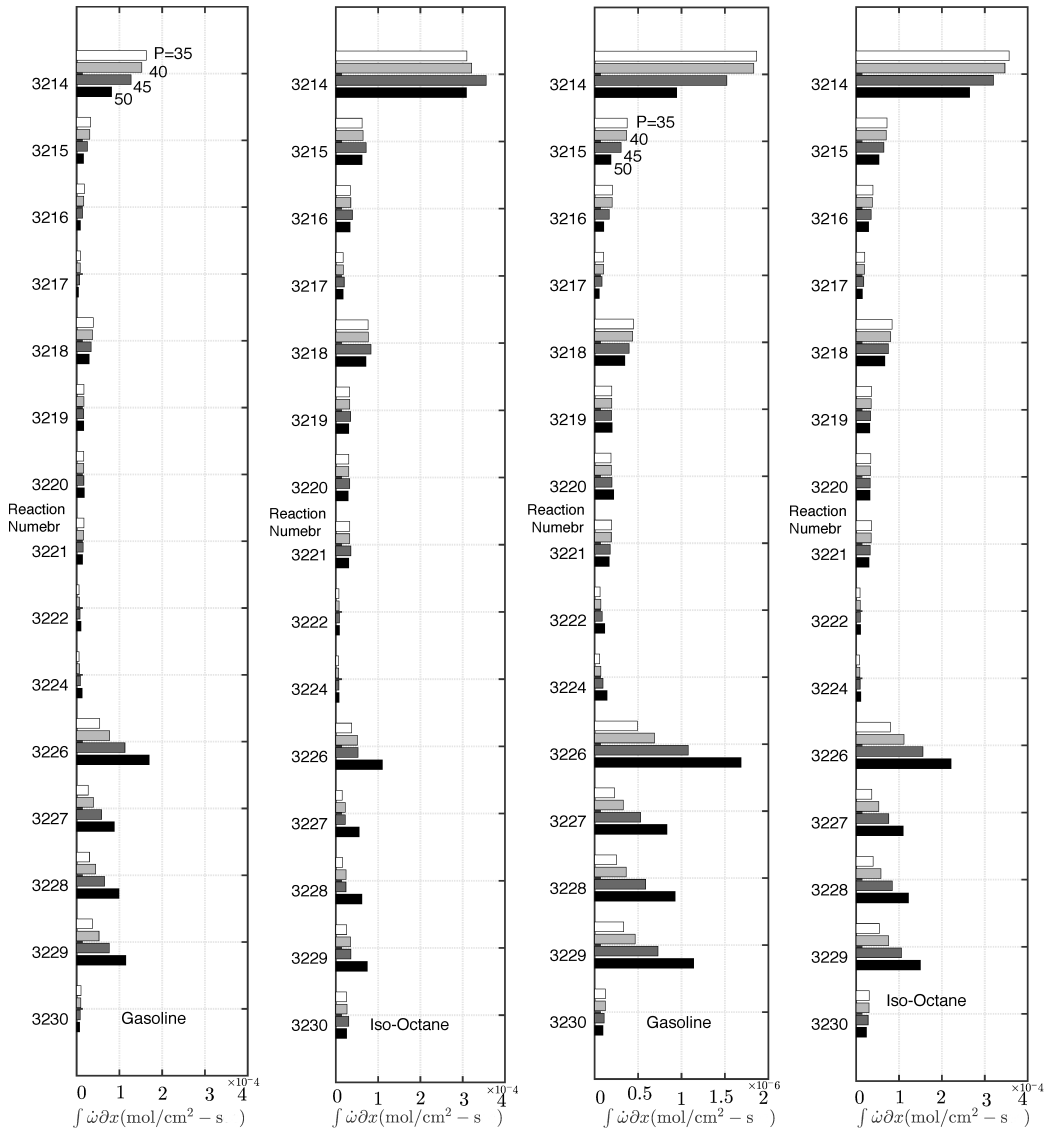

Figure 6: Net rate of elementary reaction involving iso-octane, see Table 1, integrated across the flame. The results are shown for both gasoline surrogate and iso-octane mixtures at 4 pressures, 35, 40, 45 and 50 bar, with $T_u = 850$ (left set of frames) and 900 K (right).

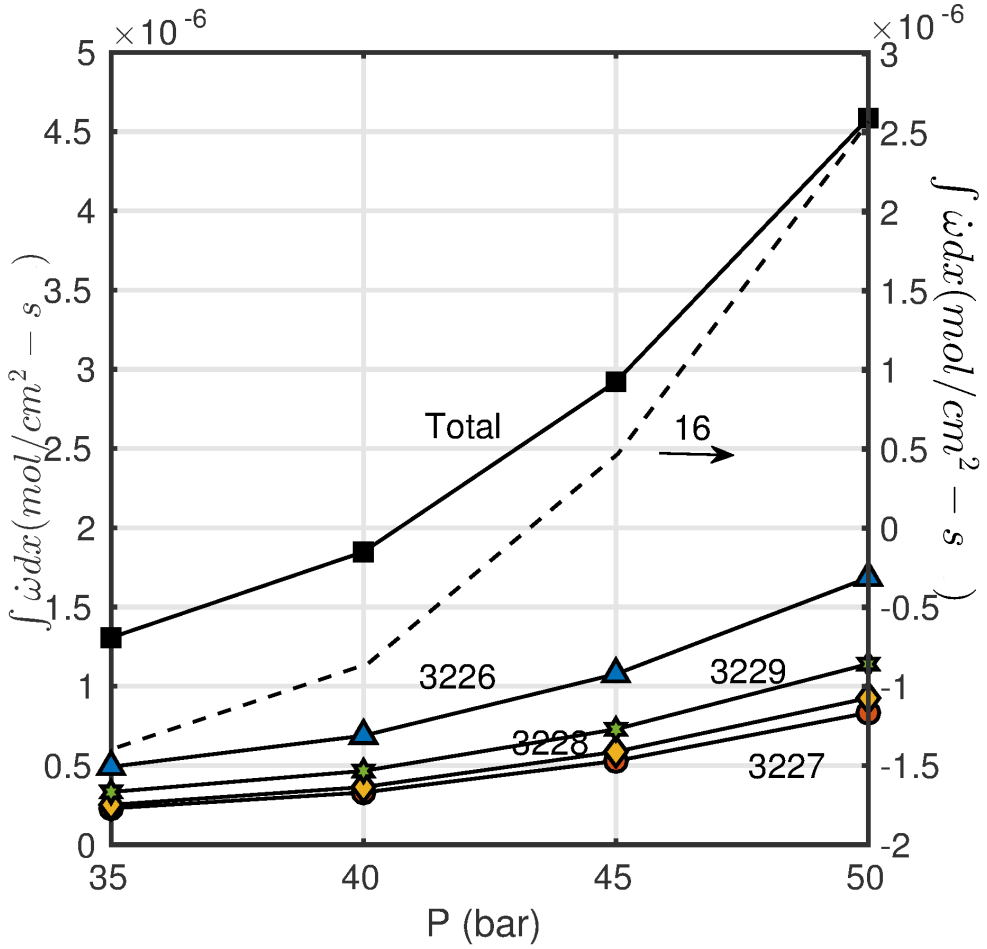

Figure 7: Variation of net reaction rate with pressure for reactions 3226 to 3229 and 16. The reaction rates are integrated across the flame for the gasoline surrogate mixture at 900 K. The reaction 16 is $H_2O_2(+M) \longleftrightarrow OH + OH(+M)$. The net rates of reactions 3226 to 3329 use the scale on the left side while reaction 16 uses the scale on the right.